

Nflation: observable predictions from the random matrix mass spectrum

Soo A Kim and Andrew R. Liddle

Astronomy Centre, University of Sussex, Brighton BN1 9QH, United Kingdom

(Dated: November 5, 2021)

We carry out numerical investigations of the perturbations in Nflation models where the mass spectrum is generated by random matrix theory. The tensor-to-scalar ratio and non-gaussianity are already known to take the single-field values, and so the density perturbation spectral index is the main parameter of interest. We study several types of random field initial conditions, and compute the spectral index as a function of mass spectrum parameters. Comparison with microwave anisotropy data from the Wilkinson Microwave Anisotropy Probe shows that the model is currently viable in the majority of its parameter space.

PACS numbers: 98.80.Cq

astro-ph/yymmnnn

I. INTRODUCTION

The Nflation model of Dimopoulos et al. [1] corresponds to a collection of uncoupled massive fields which drive inflation via the assisted inflation mechanism [2]. The existence of multiple fields is motivated by the axions of string theory, and their presence enables sufficient inflation to be obtained without using super-Planckian field values. Models of this type had first been considered by Kanti and Olive [3] and then Kaloper and Liddle [4] in the context of Kaluza–Klein models. They showed the massive fields evolve faster to the minima of their own potential and light ones later. Easther and McAllister [5] introduced random matrix theory as a way of computing the possible distribution for masses in the Nflation model. For some related constructions see Ref. [6].

It is obviously important to develop observational predictions from such models. This has been thought difficult, because in multi-field models the predictions depend in general upon the field initial conditions as well as the model parameters. Easther and McAllister [5] only studied two types of initial conditions, where either the field values or the field energy densities were equal. Neither is well motivated physically. However, in the case of an exponential mass spectrum, Kim and Liddle [7] showed that provided there were enough fields, with randomly-chosen initial conditions, the observational predictions become essentially *independent* of initial conditions again. The reason is that with enough fields, the space of possible initial conditions is well sampled by a single realization, and they named this the ‘thermodynamic regime’.

The purpose of this article is to apply the random initial conditions approach of Ref. [7] to the random matrix mass spectrum of Ref. [5], in order to explore its observational predictions and test its viability.

The main observables are the density perturbation spectral index n_s , the tensor-to-scalar ratio r , and the non-gaussianity parameter f_{NL} . Some quite general results are already known, applying to arbitrary mass spectra and initial conditions provided sufficient inflation is obtained. Alabidi and Lyth [8] showed that r always has the same value as in the single-field case, and Kim and

Liddle [9] showed that the same was true of f_{NL} (this having previously been shown for two fields in Ref. [10]). Only n_s has model and initial conditions dependence, and it has been shown that its predicted value cannot be larger than the single-field value [11, 12]. There are some further generalisations of these results [9, 12].

II. THE RANDOM MATRIX THEORY

Once one considers the scalar fields in inflation as axions in string theory, their masses can be written in matrix form, which depends on specific details on compactification (following Ref. [5], we also assume that higher-order terms can be neglected, so that what are really cosine functions can be approximated as massive uncoupled fields). The shape of the mass distribution depends only on the basic structure of the mass matrix, which is specified by the supergravity potential. In the simplest assumption, the entries in the mass spectrum are independent and identically distributed, i.e. a random matrix. The fields can be uncoupled by diagonalization of this matrix, with the mass spectrum given by the distribution of eigenvalues. The distribution of the eigenvalues for random matrices of this kind is characterized by the Marčenko–Pastur law [13] when the matrices are large. The distribution function depends on a parameter β , the ratio of the number of axions to the dimension of the moduli space. Easther and McAllister [5] devised this formalism and computed the observational predictions in terms of β for specific choices of initial conditions for the fields where the field values or the energy densities are identical (see also Ref. [14]).

We follow their notation for the mass spectrum, and label the average value of the mass-squared $\langle m^2 \rangle = \bar{m}^2$. We will throughout put $\bar{m} = 10^{-6} M_{\text{Pl}}$ where M_{Pl} is the reduced Planck mass; a simple rescaling of \bar{m} would be sufficient to match the observed normalization of perturbations. The mass spectrum is determined by two quantities, the number of fields N_f and a parameter β which governs its shape. The shape parameter β lies in the range zero to one, with values around 1/2 perhaps

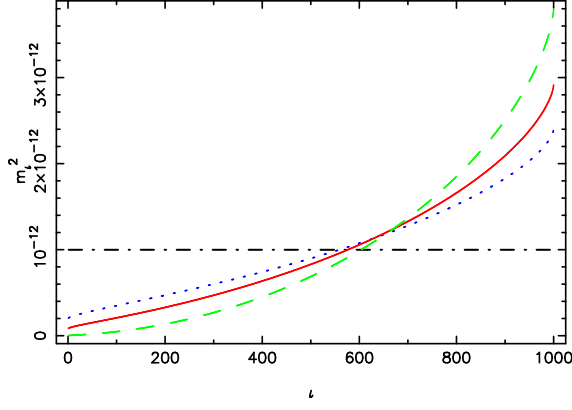


FIG. 1: The mass-squared distribution for 1000 fields; the dashed-dotted (black) flat line is for $\beta = 0$, the dotted (blue) for $\beta = 0.3$, the solid (red) for $\beta = 0.5$ and the dashed (green) for $\beta = 0.9$.

the most plausible [1, 5]. Figure 1 shows the shape of the spectrum for $N_f = 1000$ and some values of β .

III. OBSERVATIONAL PREDICTIONS

For a set of uncoupled fields with quadratic potentials, the number of e -foldings N , in the slow-roll approximation, is [11]

$$N \simeq \frac{\sum_i \phi_i^2}{4M_{\text{Pl}}^2}, \quad (1)$$

where ϕ_i is the i -th field. For our initial results, we choose the field initial values randomly from a uniform distribution in the range 0 to M_{Pl} . The total number of e -foldings is then accurately given by the linear relation $N_{\text{tot}} \simeq N_f/12$ [7], this result holding for an arbitrary mass spectrum. We will throughout assume the observable scales crossed outside the horizon 50 e -foldings before the end of inflation. Accordingly, sufficient inflation requires a minimum of around 700 fields.

In passing we note that increasing the number of fields increases the energy scale at the end of inflation, and hence might increase the number of e -foldings relevant to observable perturbations. However this effect is well within current uncertainties from the unknown behaviour of the Universe between inflation and nucleosynthesis.

We follow the usual formulae for the observational predictions of $\mathcal{P}_{\mathcal{R}}$, n_s , r , and f_{NL} . These are [5, 7, 9, 11]

$$\mathcal{P}_{\mathcal{R}} \simeq \frac{\sum_i m_i^2 \phi_i^2 \sum_j \phi_j^2}{96\pi^2 M_{\text{Pl}}^6}, \quad (2)$$

$$n_s \simeq 1 - 4M_{\text{Pl}}^2 \left[\frac{\sum_i m_i^4 \phi_i^2}{(\sum_k m_k^2 \phi_k^2)^2} + \frac{1}{\sum_j \phi_j^2} \right], \quad (3)$$

$$\simeq 1 - \frac{1}{N} - 4M_{\text{Pl}}^2 \left[\frac{\sum_i m_i^4 \phi_i^2}{(\sum_k m_k^2 \phi_k^2)^2} \right], \quad (4)$$

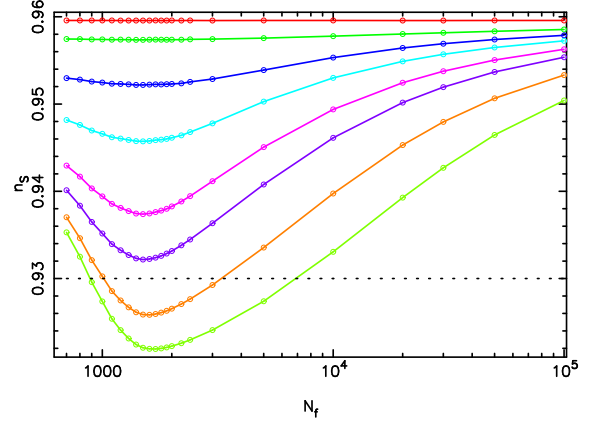


FIG. 2: The spectral index n_s (from top to bottom, $\beta=0, 0.1, 0.3, 0.5, 0.7, 0.8, 0.9$ and 0.95). The dotted line shows the observational lower limit on n_s from WMAP3.

$$r \simeq \frac{32M_{\text{Pl}}^2}{\sum_i \phi_i^2} \simeq \frac{8}{N}, \quad (5)$$

$$-\frac{5}{6}f_{\text{NL}}^{(4)} \simeq \frac{2M_{\text{Pl}}^2}{\sum_i \phi_i^2} \simeq \frac{1}{2N} \simeq \frac{r}{16}, \quad (6)$$

where m_i and $f_{\text{NL}}^{(4)}$ are the i -th mass and the second term of the nonlinearity parameter f_{NL} respectively (the first contribution to f_{NL} is model-independent and small [15, 16]). More detailed calculations of the non-gaussianity have confirmed that this is the leading contribution to the non-gaussianity [17]. We have simulated these observables and will show in particular n_s to study the effect from this mass distribution.

A. The spectral index

The most important observable in Nflation models is the spectral index, which we calculated as described above and show in Fig. 2. We see that it depends on both model parameters N_f and β .

The curves have a generic shape where they first dip, and then, after a minimum typically around $N_f = 1500$, increase to join the single-field value. The single-field value is always obtained in the case $\beta = 0$, in which all masses become identical and this result is well known (e.g. Ref. [11]). These curves look a little different from Fig. 4 in Ref. [7], studying an exponential mass spectrum where the values asymptoted to constants for large N_f . This is just because N_f is defined here in a rather different way; in Ref. [7] increasing it added new fields at the top of the mass range, and if they were heavy enough they fell to their minima before observable scales left the horizon. The distinction here is that when we increase N_f we are packing more fields into the same mass interval, forcing us to the equal-mass case. That the curves begin to rise after $N_f \simeq 1500$ indicates that fields heavier than the 1500th have typically reached their vacuum state before

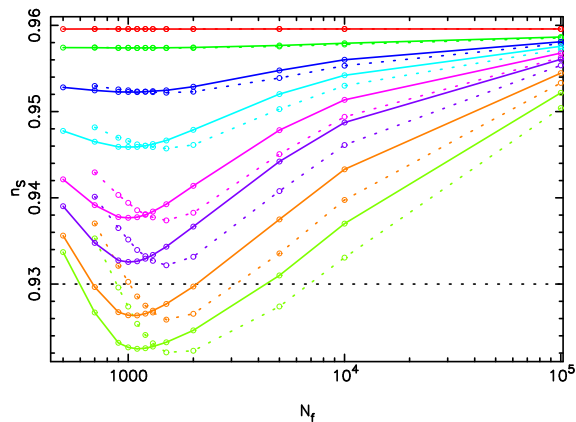


FIG. 3: As Fig. 2, but now showing sets of curves for two choices of initial condition distributions. The dashed lines reproduce the curves from Fig. 2, and the solid ones show initial conditions with ϕ_i^2/M_{Pl}^2 drawn from a uniform distribution.

the 50 e -foldings point.

To compare with observations, the analysis in Ref. [16] shows that for $r = 8/50$, the 95% confidence lower limit for n_s lies at about 0.93, shown as the dotted line in the figure. Provided $\beta \leq 0.8$, the spectral index is always large enough regardless of the number of fields. For large β , the model is excluded only for a range of N_f running from about one thousand to several thousand. Accordingly, most of the model parameter space is currently viable.

The results shown in Fig. 2 are the mean values over realizations of the initial conditions. Additionally we find that the spread in n_s values is quite small; the standard deviation of n_s is never more than one percent of its displacement from unity. This confirms the existence of the thermodynamic regime for this mass spectrum, just as in Ref. [7].

Although the above analysis shows that for our chosen initial distribution, the observational predictions are independent of realization, one might further ask whether there is dependence on the choice of that distribution. In order to test that, we carried out two further series of simulations. In the first series, we took ϕ_i^2/M_{Pl}^2 to be chosen uniformly between zero and one. The results are shown in Fig. 3. The curves are shifted to a smaller number of fields, retaining both their shape and minima. We found that when the number of fields is multiplied by 3/2, making the total number of e -foldings the same, these solid curves become matched to the dotted ones. This can be related to the different initial distributions by an approximate analytic argument given in the Appendix.

In the second series, we chose the field energy densities to be uniformly distributed, with the lightest field ranging from 0 to M_{Pl} and the other fields given smaller ranges to ensure the same expected energy density. This is distinct from Ref. [5] who gave each field the *same* energy density, rather than the same only on average.

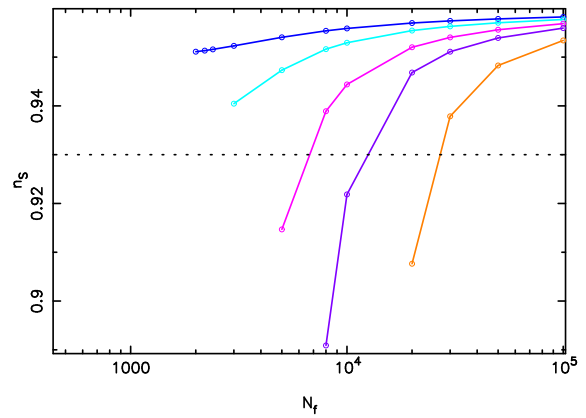


FIG. 4: As Fig. 2, but showing results for uniformly-chosen field energy densities. Only $\beta = 0.3, 0.5, 0.7, 0.8$ and 0.9 (from top to bottom) are shown. The left-hand end of the curves corresponds to models only just achieving 50 e -foldings in total.

In this case the more massive fields start closer to their minima, and a greater total number of fields is needed to get sufficient inflation. The results are shown in Fig. 4. The curves have a rather different shape, and there is some difficulty in achieving a minimum of 50 e -foldings unless N_f is large. The analytic analysis given in the Appendix does not apply in this case, as the field initial values are correlated to the masses. Nevertheless the overall conclusion is the same: that only for large β is there a danger that the models are ruled out through predicting too small a value for n_s , and even then only in a narrow range of N_f . The expected value $\beta \simeq 0.5$ is therefore viable for all initial condition distributions we tested.

B. Other observables

Concerning the tensor-to-scalar ratio r and the non-gaussianity parameter f_{NL} , unsurprisingly the results are same as in our previous work [7, 9]. Comparing to the analytical results of Eqs. (5), (6), we confirm numerically that r is indeed independent of the model parameters, $r = 0.16$, and that $f_{\text{NL}} \simeq 2/N$ which will never be sufficiently large to be detected. All simulations of r and f_{NL} individually give those results, without needing to average over realizations of the initial conditions.

IV. CONCLUSIONS

We have carried out a detailed numerical investigation of the inflationary perturbations in Nflation models with the mass spectrum of random matrix theory. We produced the predictions for the spectral index as a function of both the number of fields N_f and the distribution parameter β in the mass spectrum. We have found that

the model remains viable in the majority of its parameter space, and that the thermodynamic regime, where the predictions become independent of the initial condition realization, holds for this spectrum as for the exponential case [7].

Acknowledgments

A.R.L. was supported in part by PPARC (UK). S.A.K. acknowledges the hospitality of Filippo Vernizzi and the Abdus Salam ICTP in Italy, and A.R.L. of the Institute for the Astronomy, University of Hawai'i, while part of this work was being carried out. We thank Richard Easther for providing his code generating the MP mass spectrum, and for many discussions relating to this work including the analytic evolution formulation described in the Appendix.

APPENDIX: ANALYTIC EVOLUTION

This appendix is based on unpublished work by Richard Easther, whom we thank for providing details.

In the main text we considered different initial distributions for the scalar fields. When the initial values of ϕ_i/M_{Pl} and ϕ_i^2/M_{Pl}^2 are randomly chosen uniformly between zero and one, the expectation value $\alpha \equiv \langle \phi_i^2/M_{\text{Pl}}^2 \rangle$ is 1/3 and 1/2 respectively (other choices will give a different α). Eq. (1) becomes $N_{\text{tot}} \simeq N_f \alpha/4$. This difference by a factor 2/3 is closely related to the shift in the curves shown in Fig. 3.

This can be shown via an analytic approximation to the evolution, in order to extract estimates of the summations $\sum_i^{N_f} m_i^2 \phi_i^2$ and $\sum_i^{N_f} m_i^4 \phi_i^2$ which appear in the expression for the spectral index. Using the slow-roll approximation, the field value is

$$\phi_i(t) = \phi_i(t_0) \tau^{m_i^2/b}(t), \quad (7)$$

where $\tau(t)$ and b have the same definition as in Ref. [5]: they are the ratio of the value of the heaviest field at the time t to its initial value, and the upper limit of the probability distribution of the mass-squared spectrum, respectively. Also t_0 is the initial time. Then using the exponential function with $c = c(t) \equiv 2 \ln[\tau(t)]/b$, we can rewrite the summation terms such as

$$\sum_i^{N_f} m_i^2 \phi_i^2(t) = \sum_i^{N_f} m_i^2 \phi_i^2(t_0) \exp[m_i^2 c]. \quad (8)$$

If one ignores correlations between the mass distribution and the initial field distribution, so that $\langle m_i^2 \exp[m_i^2 c] \phi_i^2(t_0) \rangle = \langle m_i^2 \exp[m_i^2 c] \rangle \langle \phi_i^2(t_0) \rangle$, then with the Marčenko–Pastur distribution, the expectation value is given by

$$\langle x^i \rangle = \bar{x}^i {}_2F_1(1-i, -i; 2; \beta), \quad (9)$$

where ${}_2F_1$ is the hypergeometric function. This follows from Eq. (6.14) of Ref. [5], where the summation can be rewritten as a hypergeometric function.

Therefore the summation terms with the expectation values of field initial conditions and of distribution of mass spectrum are

$$\sum_i^{N_f} m_i^2 \phi_i^2(N) \quad (10)$$

$$= 4N_{\text{tot}} M_{\text{Pl}}^2 \bar{m}^2 \sum_{i=0}^{\infty} \bar{m}^{2i} {}_2F_1(-i, -i-1; 2; \beta) \frac{c^i}{i!},$$

$$\sum_i^{N_f} m_i^4 \phi_i^2(N) \quad (11)$$

$$= 4N_{\text{tot}} M_{\text{Pl}}^2 \bar{m}^4 \sum_{i=0}^{\infty} \bar{m}^{2i} {}_2F_1(-i-1, -i-2; 2; \beta) \frac{c^i}{i!}.$$

Note that t is related to $N_{\text{tot}} - N$; that is, t counts forward from when the fields start to evolve from their own initial conditions, while N is the number of e -foldings before the end of inflation.

The n_s data in Fig. 3 are taken at different times, but at the same N . Using Eqs. (10) and (11), the n_s formula becomes

$$n_s \simeq 1 - \frac{1}{N} - \frac{f(t, \beta)}{N_{\text{tot}}}, \quad (12)$$

where

$$f(t, \beta) \equiv \frac{\sum_i^{\infty} \bar{m}^{2i} {}_2F_1(-i-1, -i-2; 2; \beta) c^i / i!}{\left[\sum_j^{\infty} \bar{m}^{2j} {}_2F_1(-j, -j-1; 2; \beta) c^j / j! \right]^2}. \quad (13)$$

Here the function $f(t, \beta)$ represents how n_s evolves with respect to time (or N). Even though it is hard to evaluate it in general, it will have the same value whenever t and β are same. Hence in cases with same N_{tot} , but not necessarily the same N_f or α , then n_s must be same. This explains why the solid curves in Fig. 3 are matched with dotted ones after multiplying 3/2 to N_f , because this makes N_{tot} the same. Different α shifts the n_s curves along the N_f axis, with bigger α shifting the curves in the smaller N_f direction.

We can conclude then that, insofar as the approximations hold, $\beta \lesssim 0.8$ should satisfy the current observations regardless of the field initial condition distribution, while for larger β some choices of N_f will be ruled out and that those N_f values depend on the α value of the initial condition distribution. However the above analysis relies on using a slow-roll approximation for all fields, which is likely to become increasingly inaccurate as increasing numbers of fields evolve towards their minima, and assumes the mass and initial field value distributions to be uncorrelated. The latter approximation fails badly for the uniform field energy density initial conditions.

-
- [1] S. Dimopoulos, S. Kachru, J. McGreevy, and J. Wacker, hep-th/0507205.
 - [2] A. R. Liddle, A. Mazumdar, and F. E. Schunck, Phys. Rev. D **58**, 061301(R) (1998), astro-ph/9804177.
 - [3] P. Kanti and K. A. Olive, Phys. Rev. D **60**, 043502 (1999), hep-ph/9903524; P. Kanti and K. A. Olive, Phys. Lett. B **464**, 192 (1999), hep-ph/9906331.
 - [4] N. Kaloper and A. R. Liddle, Phys. Rev. D **61**, 123513, (2000), hep-ph/9910499.
 - [5] R. Easther and L. McAllister, JCAP **0605**, 018 (2006), hep-th/0512102.
 - [6] A. Jokinen and A. Mazumdar, Phys. Lett. B **597**, 222 (2004), hep-th/0406074; K. Becker, M. Becker, and A. Krause, Nucl. Phys. B **715**, 349 (2005), hep-th/0501130.
 - [7] S. A. Kim and A. R. Liddle, Phys. Rev. D **74**, 023513 (2006), astro-ph/0605604.
 - [8] L. Alabidi and D. H. Lyth, JCAP **0605**, 016 (2006), astro-ph/0510441.
 - [9] S. A. Kim and A. R. Liddle, Phys. Rev. D **74**, 063522 (2006), astro-ph/0608186.
 - [10] F. Vernizzi and D. Wands, JCAP **0605**, 019 (2006), astro-ph/0603799.
 - [11] D. H. Lyth and A. Riotto, Phys. Rep. **314**, 1 (1999), hep-ph/9807278.
 - [12] Y.-S. Piao, Phys. Rev. D **74**, 047302 (2006), gr-qc/0606034.
 - [13] V. A. Marčenko and L. A. Pastur, Math. USSR. Sbornik **1**, 457 (1967).
 - [14] J.-O. Gong, Phys. Rev. D **75**, 043502 (2007).
 - [15] J. M. Maldacena, JHEP **0305**, 013 (2003), astro-ph/0210603.
 - [16] D. N. Spergel et al. (WMAP Collaboration), Astrophys. J. Supp. **170**, 377 (2007), astro-ph/0603449.
 - [17] T. Battefeld and R. Easther, JCAP **0703**, 020 (2007), astro-ph/0610296; D. Battefeld and T. Battefeld, JCAP **0705**, 012 (2007), hep-th/0703012.